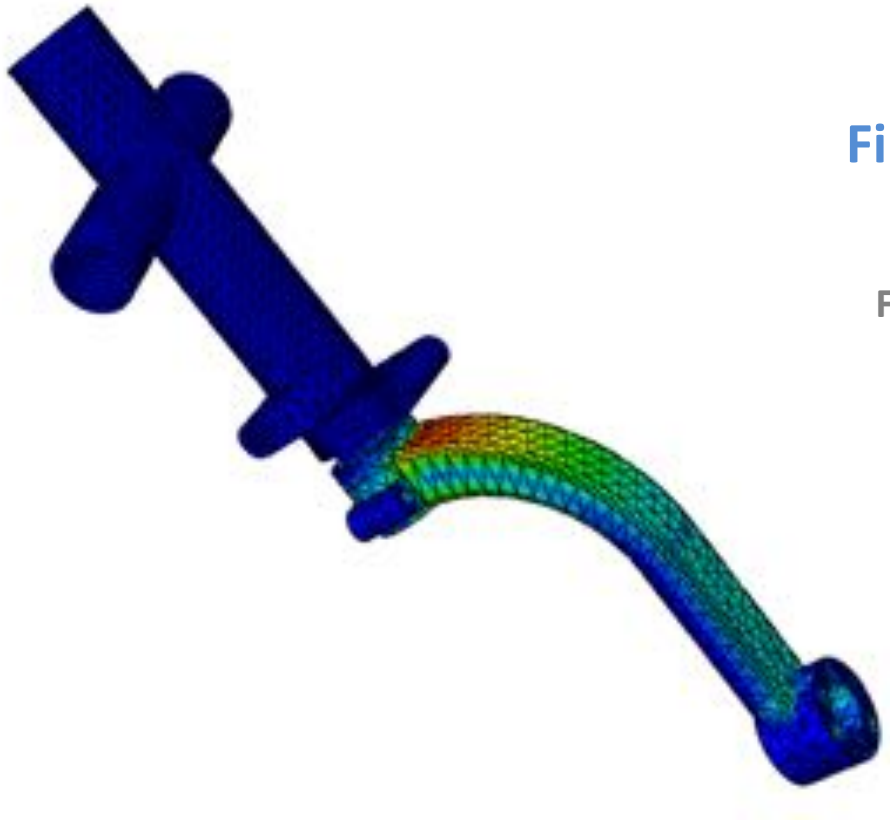

ME 461:
Finite Element Analysis

Fall | 2015

A Semester Report on:

The Development and Analysis of a Nose Landing Gear

Group Members:

Blake Maloney, Khaled Alroumi, Robert Mitchell

PennState
College of Engineering

Department of Mechanical and Nuclear Engineering, University Park, PA

Table of Contents

Executive Summary

To determine potential failure locations in an aircraft landing gear using finite element analysis. Considerations in our analysis will include aircraft speed and aircraft weight.

Background

An aircraft's landing gear is subjected to extreme forces during a landing. The energy must be properly dissipated throughout the entirety of the landing gear to ensure a safe end to an aircraft's journey. Our project would focus on potential areas of failure within the system of the landing gear. This will include an analysis of geometric stress concentrations that could be problematic under loading.

General Approach

The first step in our analysis will be to select a specific aircraft and landing gear to model. Next, we would need to research the aircraft to find information such as weight distribution, material selection, and loading capabilities. We will then need to create a 3-D model of the landing gear based on aircraft schematic diagrams. Once the 3-D model is created, we will create a mesh and choose element types that will highlight where the greatest stresses and potential areas of failure will be. After creating a mesh, we will need to determine the forces acting on the landing gear and the boundary conditions. Finally, the loading conditions and mesh will be used in combination to determine the stress in all areas of the landing gear.

Acknowledgements

We would like to thank Dr. Reuben Kraft for all of his help throughout the duration of this project.

List of Figures

Section 1: Background and Project Plan

Material Properties for nose landing gear:

The metal components of the landing gear will be Ti-6Al-4V, which is typical for most landing gears, especially those used for smaller planes, such as the Piper Arrow we are analyzing.

Table 1: Ti-6Al-4V Material Properties

Property	Value
Brinell Hardness	334
UTS	950 MPa
Tensile Yield Strength	880 MPa
Modulus of Elasticity	113.8 GPa
Compressive Yield Strength	970 MPa
Poisson's Ratio	0.342
Fracture Toughness	75 MPa-$m^{1/2}$
Shear Modulus	44 GPa
Shear Strength	550 MPa

Constitutive Equations utilized will just be the force balance for the landing gear, taking into account weight and many factors described below. From the loading conditions, we will then utilize stress/strain relationships, equations such as Hooke's Law and Poisson's Ratio, to determine the stress in the landing gear.

Determination of Forces

- **Ground Forces:** This is the reaction force acting on the landing gear when it comes into contact with the ground. In this analysis we will apply the load directly to the wheel rather than including the tire in the analysis, due to the complexity of the tire deformation. The force on the tire will be accounted for by applying a distributed pressure force along the tire-wheel interface, due to the inflation of the tire at landing point. The inflation pressure will not very much throughout landing, so it will be assumed constant. The weight of the plane we are analyzing is 1,798 lbs with no one inside. We will estimate the plane's weight as 2000 lbs, assuming one person as the pilot. From this weight, the ground vertical force can then be determined using Figure 1 and Equation 1, both found in Reference 1.

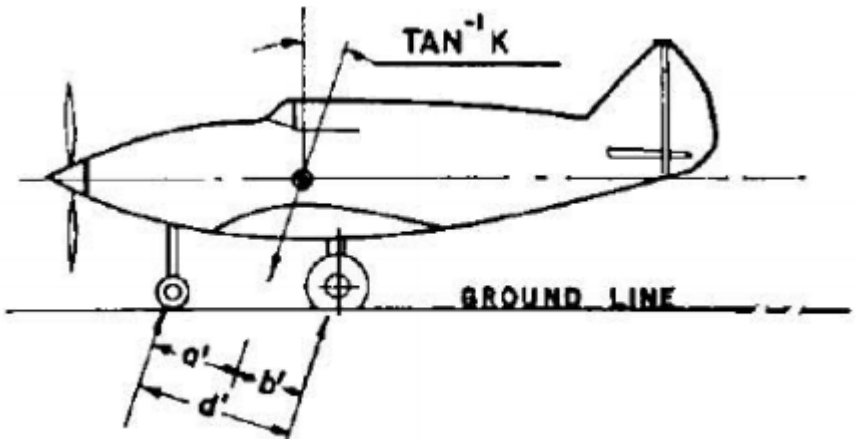

Figure 1: Level landing with inclined reactions.[2]

$$V_f = (n - L) \cdot W \cdot \frac{b'}{d'} \qquad (1)$$

Where b' and d' represent their respective dimensions in the drawing, W is the weight of the plane, V_f is the vertical ground force, n is the ratio of external applied vertical forces to the weight, and L is the lift to weight ratio. Because the plane examined in the reference and our plane are nearly identical, and there is not much information readily available about this plane, n, L, b', and d' will be utilized from reference 1.

$$V_f = (2.67 - 0.67) \cdot 2000 \cdot \frac{52.81}{169.51} = 124.62\ lb = 554.3N$$

- **Drag Force:** The drag force will be considered negligible compared to the ground reaction forces and because of the complexity of fluid analysis for FEA.

- Other forces and loading factors will most likely be factored into the analysis and determined as we move further into the project.

Section 2: Development and Description of the CAD Geometry

When the time came to obtain a CAD model, we had two options. The first was to create a simplified model of a piper plane landing gear. The second was to find an open source CAD file, which could be more complex than we could come up with in such a short period of time. We did some research and found a CAD assembly, Figure 2, which was obtained from Reference 1 and consisted of all different parts of a piper plane landing gear. Next, we needed to create an engineering drawing with the most important dimentions. Eventually, we needed to simplify the CAD geometry to achieve compatibility with Abaqus. This simplified CAD engineering drawing can be seen in Figure 4. Once this was done, we could move on to the meshing stage.

Figure 2: CAD assembly of a piper plane landing gear.

Figure 3: The Piper Arrow IV plane and the landing gear under analysis.

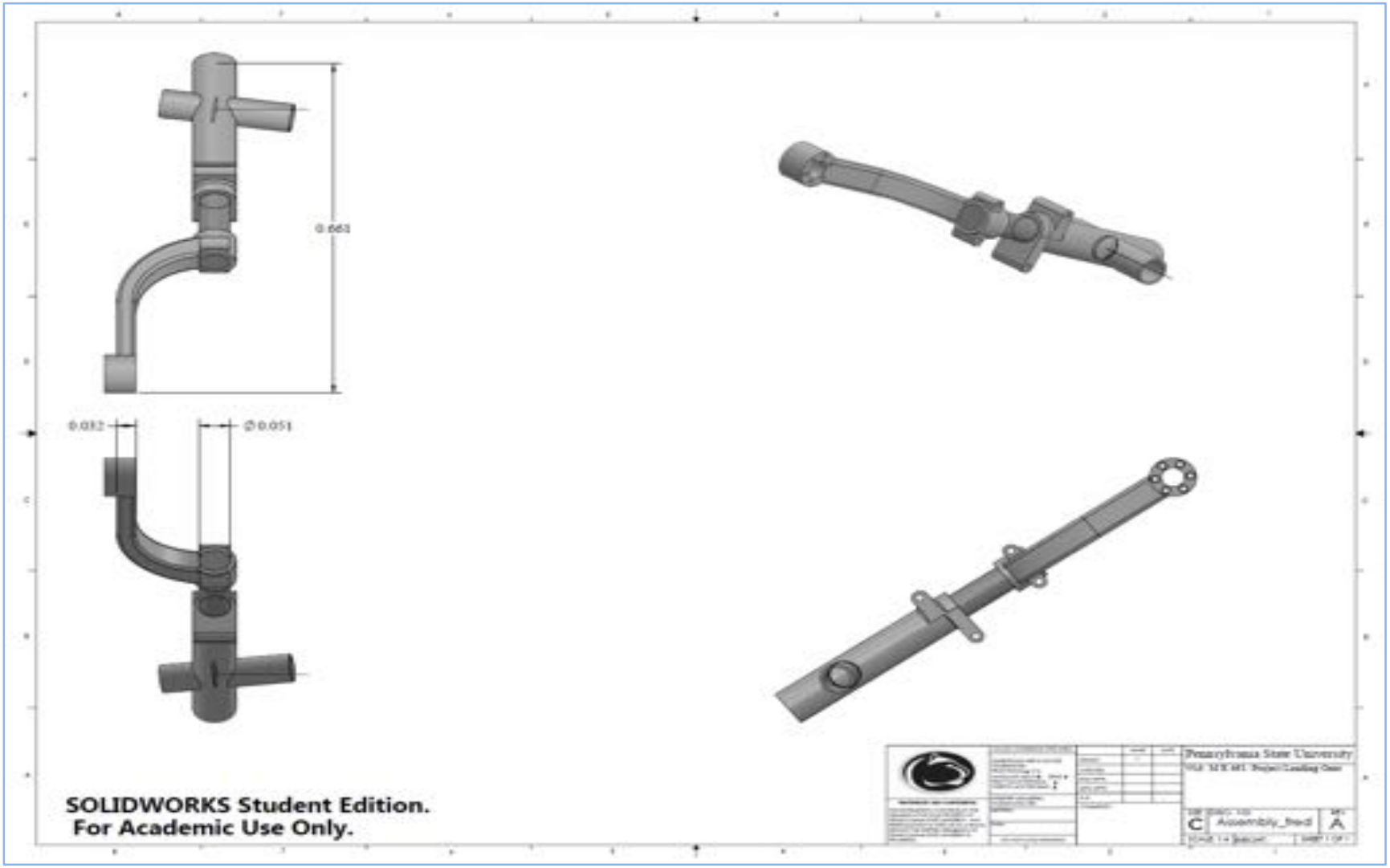

Figure 4: CAD engineering drawing of simplified landing gear assembly.

Section 3: Development of Finite Element Meshes

The next step to developing the FEA of the landing gear was to mesh all of the parts. Once we imported all of the parts into abaqus and attempted meshing and assembly, we encountered a number of problems. The first issue was that the geometries of the parts were too complex for abaqus to mesh. Upon importing the parts into Abaqus, we received the error message, "The part contains imprecise geometry, which is highlighted. Partitioning and quad/hex meshing using the medial axis algorithm may fail on imprecise parts." An example of these errors is visible in Figure 5, which highlights the imprecise geometries of the landing gear fork.

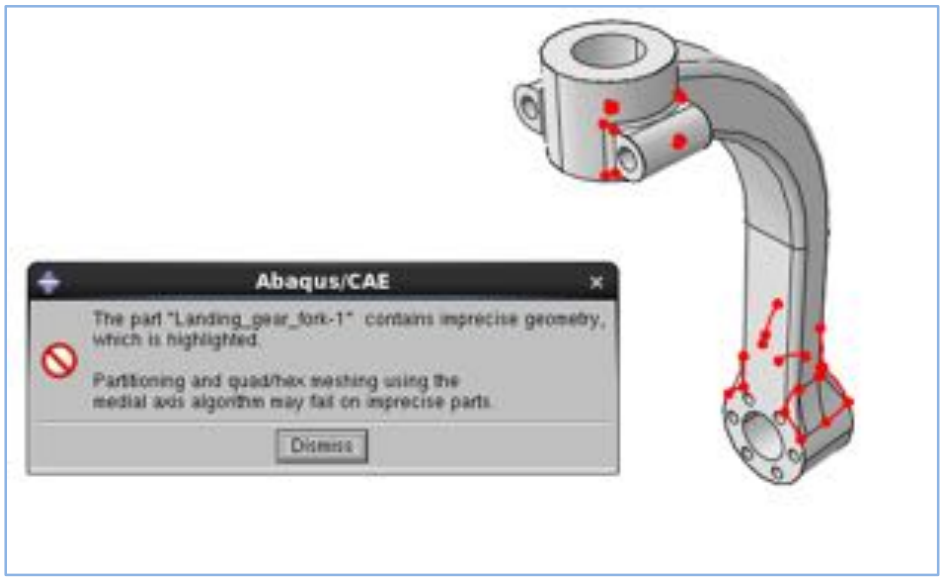

Figure 5: Abaqus error regarding imprecise part geometry.

After receiving errors concerning part geometry, we edited the SolidWorks model and removed features such as fillets and chamfers. Once the parts were updated, we were able to successfully import them into Abaqus without any errors. The simplified model of the landing gear fork and its mesh can be seen in Figure 6.The two remaining parts and their meshes can be seen in Figure 7.

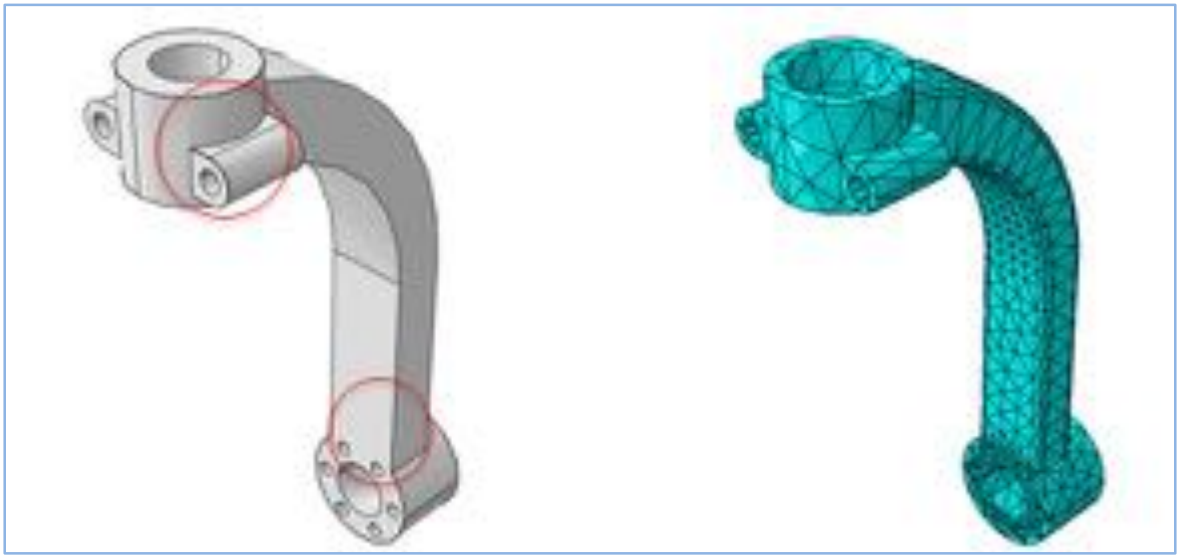

Figure 6: The updated model of the landing gear fork with its simplified features circled (left) and the meshed fork with tetrahedral elements (right).

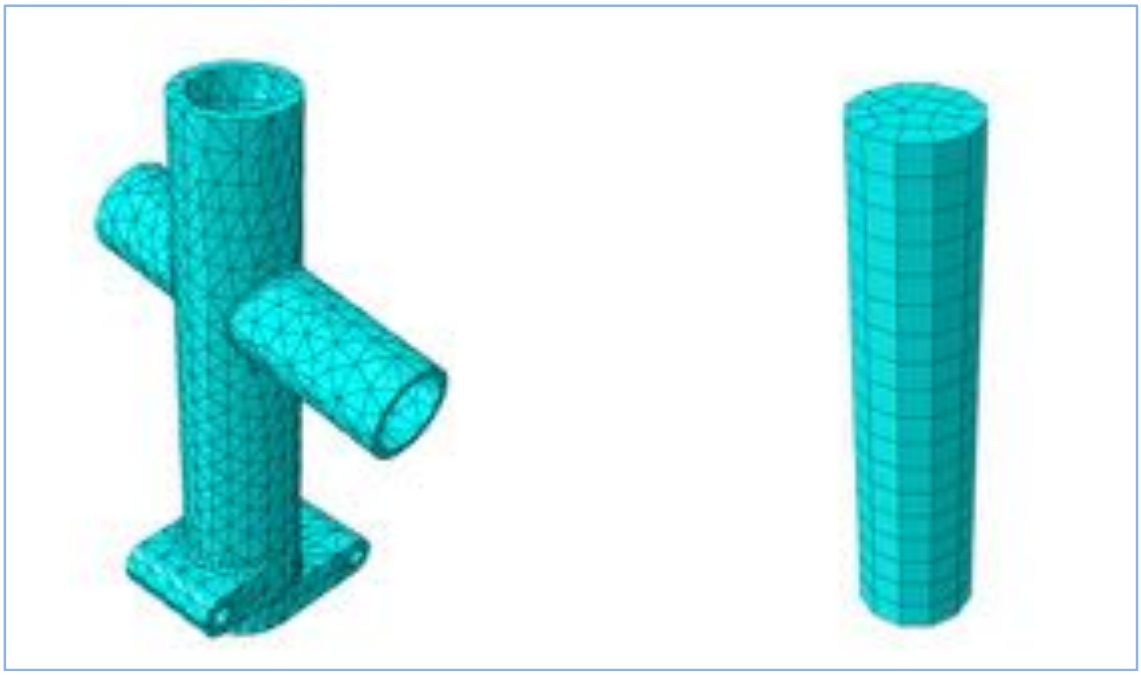

Figure 7: The meshed models of the simplified piston and cylinder.

Section 4: Development and Description of the Model Assembly and Boundary Conditions

Once the individual parts were meshed, we assembled the full model. We began by assembling two of the three instances relative to one another. The ideal two parts to do this were the damper and the landing gear fork as that constraint was the simplest. After choosing the two parts, we then added a co-axial constraint on the damper's outer surface and the hole within the landing gear fork. Once that was done, a face-to-face constraint was added to the bottom of the damper and the bottom of the hole in the landing gear fork.Once that was done, the top part of the landing gear was added to the assembly and given a co-axial constraint with the damper. A displacement then was added between the top of the damper and the bottom of the top part where the bottom of the top part was a small distance below the top of the damper. The assembly steps of the process are illustrated in Figure 8. The complete meshed assembly can be seen in Figure 9.

Figure 8: The landing gear fork and cylinder assembly (left) and the complete assembly of the landing gear (right).

Figure 9: The complete assembly of all landing gear parts with the mesh displayed.

Once the part was assembled and meshed, we applied the boundary conditions and load due to landing. A fixed boundary condition was applied to the three circular surfaces at the end of each cylinder near the top of the landing gear. This is because these parts that attach to the base of the plane, leading to a nearly rigid attachment. Another boundry condition was added to the bottom of the damper to hold it together with the top of the landing gear. Essentially, this boundary condition allows the fork and cylinder to be treated as one part. The vertical force of 555N, determined in the "Background and Project Plan," was applied as a distributed load along the the bottom of the landing gear fork. This loading condition simulates the propagation of the vertical force from the wheel to the fork. Visualizations of the boundary conditions and applied load are available in Figures 10 and 11, respectively.

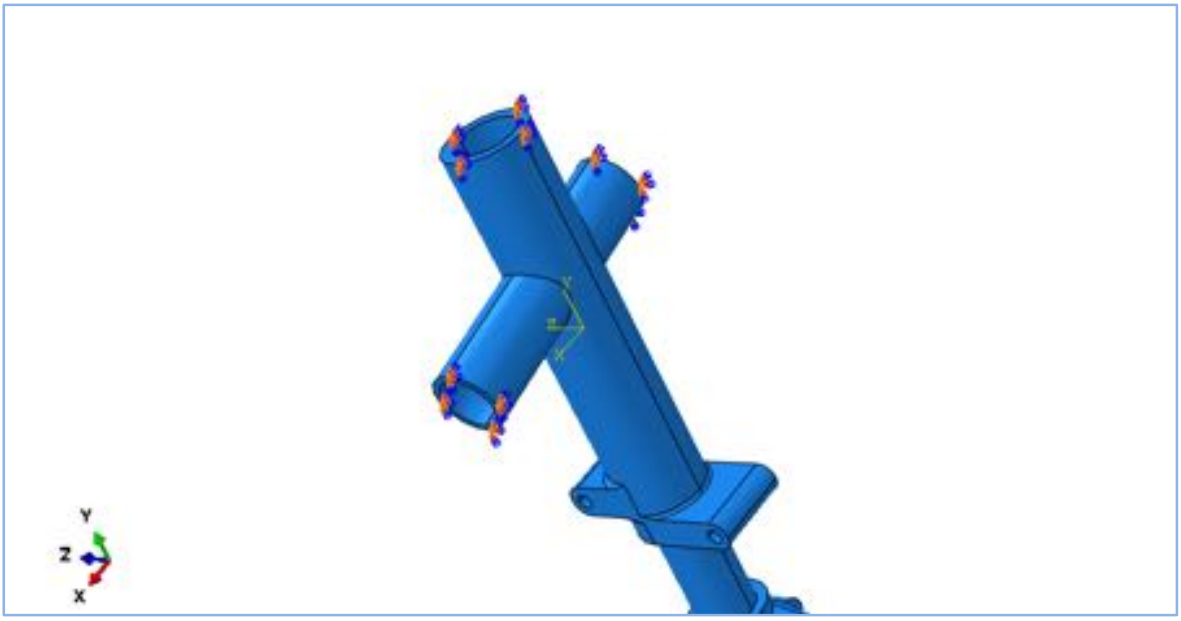

Figure 10: Boundary conditions applied to the landing gear. The three circular surface areas are fixed because they are attached to the bottom of the plane.

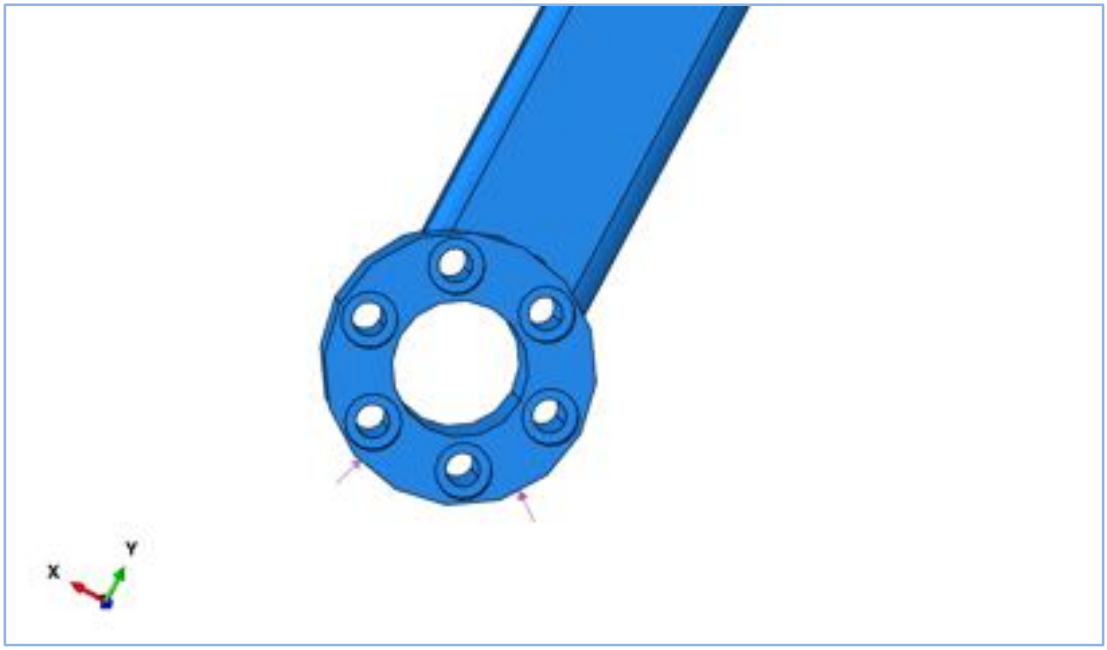

Figure 11: Vertical force of 555N due to landing applied to the landing gear fork.

Section 5: Development and Description of Model Interactions

Once the boundary conditions and loading were applied to the landing gear, the only model interaction that needed to be added was between the damper and cylinder. In an actual, unsimplified landing gear, the interaction between these two parts is a hydraulic piston-cylinder interaction. Due to the complexity of this interaction, and the fluid mechanics involved, we simplified it as a friction interaction. The friction formulation was a penalty approach and the corresponding friction coefficient was 1.35. This interaction, displayed in Figure 12, was created between the outer surface of the damper and the inner surface of the hollow cylinder.

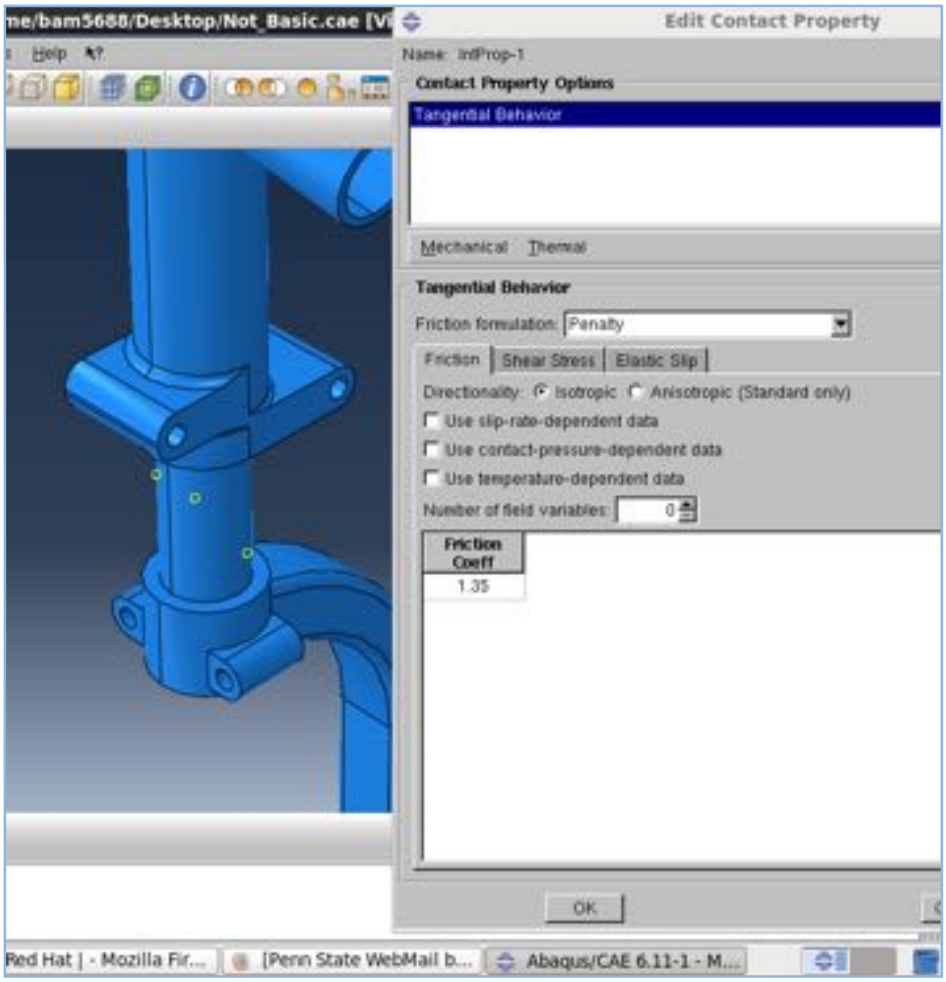

Figure 12: The friction interaction created between the damper and hollow cylinder.

Section 6: Analysis of Finite Element Model

With the boundary conditions and loading applied, we simply applied the material conditions for Ti-6Al-4V, listed in Table 1, to all parts of the landing gear and then ran the simulation. The job took approximately 15-20 seconds to run and produced the results shown in Figures 13 and 14.

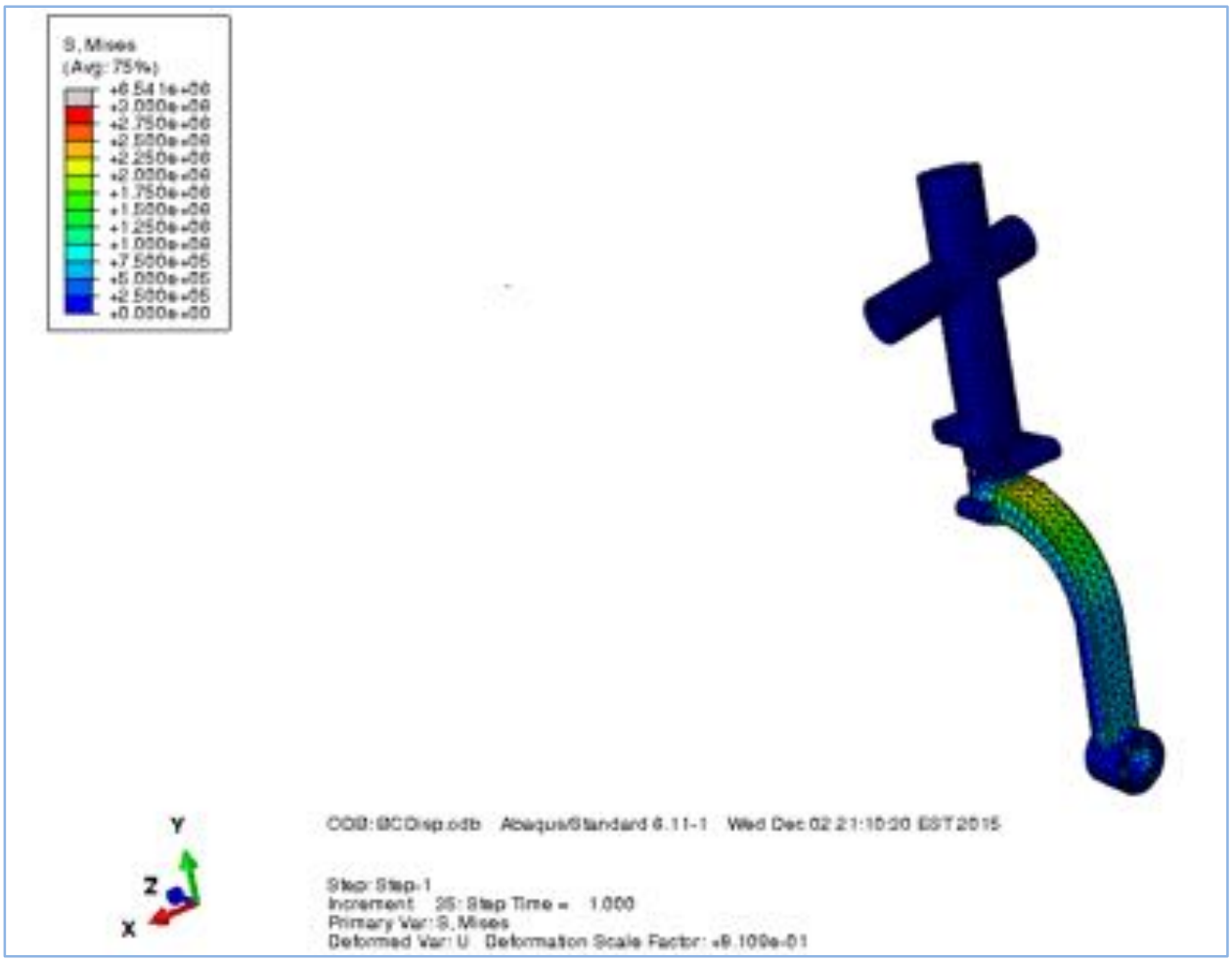

Figure 13: Front view of resultant stress contours with all boundary conditions, loading, and property interactions completed.

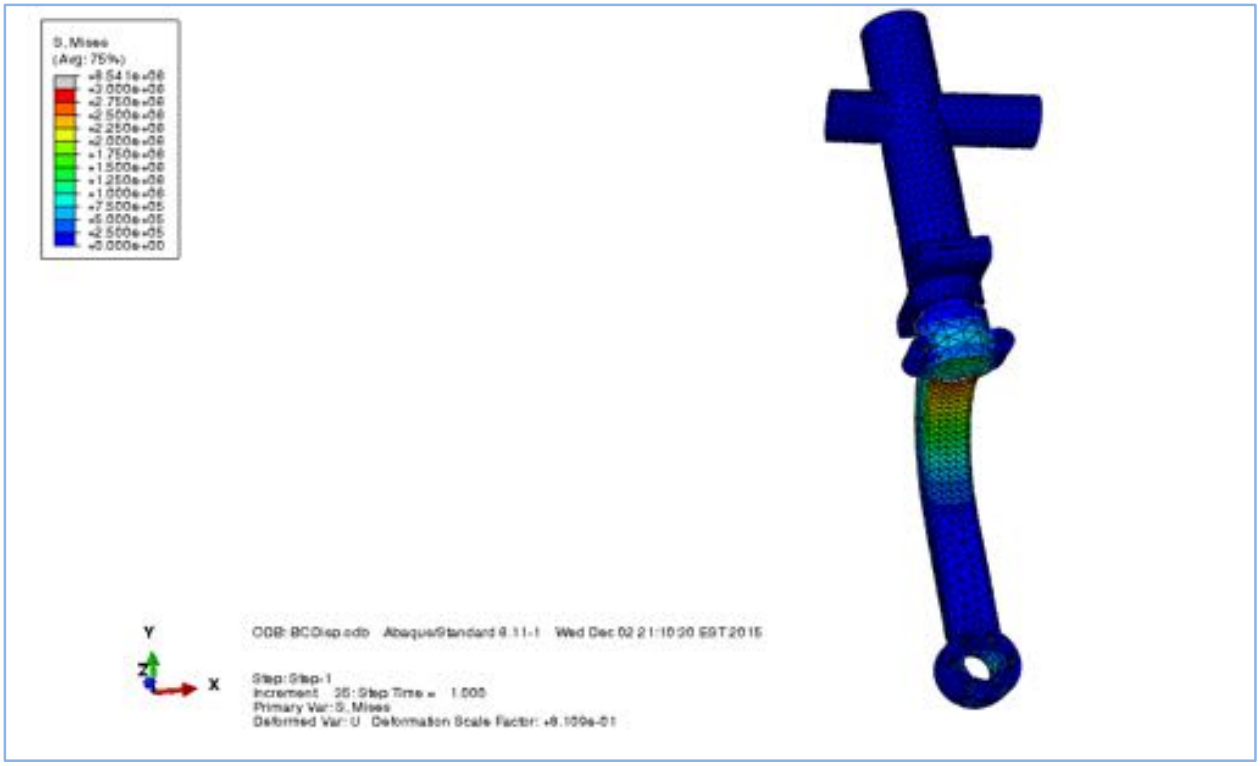

Figure 14: Back view of resultant stress contours with all boundary conditions, loading, and property interactions completed.

The resultant maximum Von Mises stress was 6.54 MPa and occurred near the top of the landing gear fork. This resultant stress is on a realistic order of magnitude and is located at a geometric stress concentration. The variation of the stress along the landing gear fork was highlighted using a path, shown in Figure 15. The stresses at the corresponding path points are displayed in Figure 16. The graph in Figure 16 shows that the stress peaks at the stress concentrations at the top of the landing gear fork, and decreases near the bottom of the fork.

A modal analysis was also performed during the simulation to find the natural frequencies. The results of the modal analysis are shown in Figure 17.

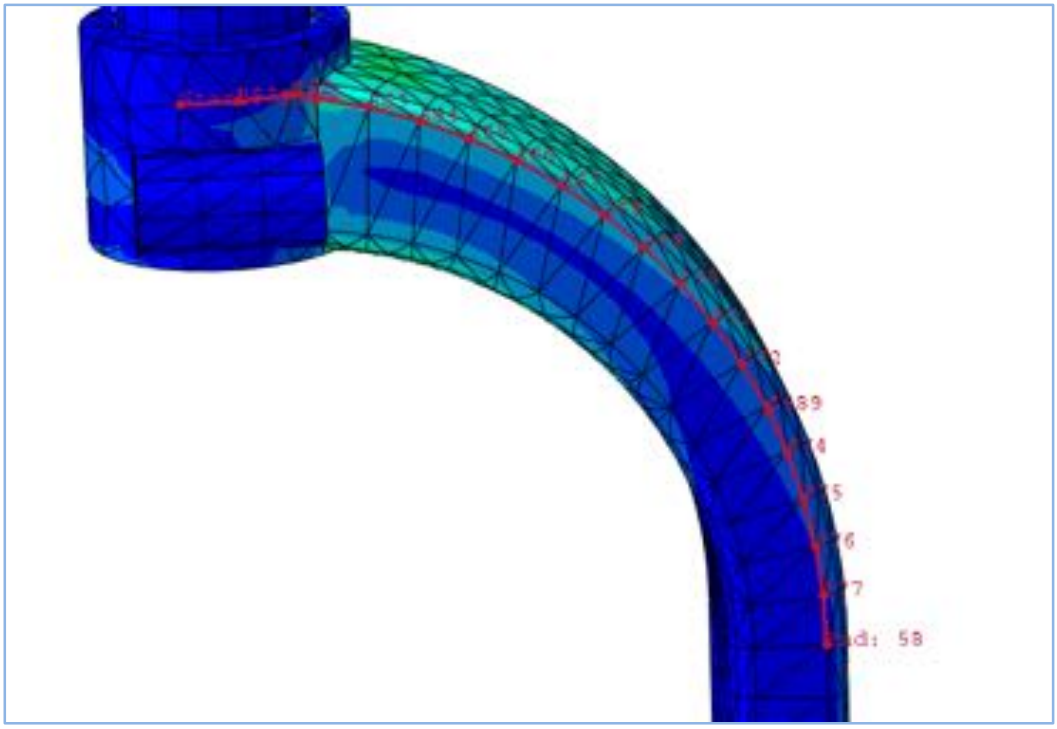

Figure 15: Point path along the landing gear.

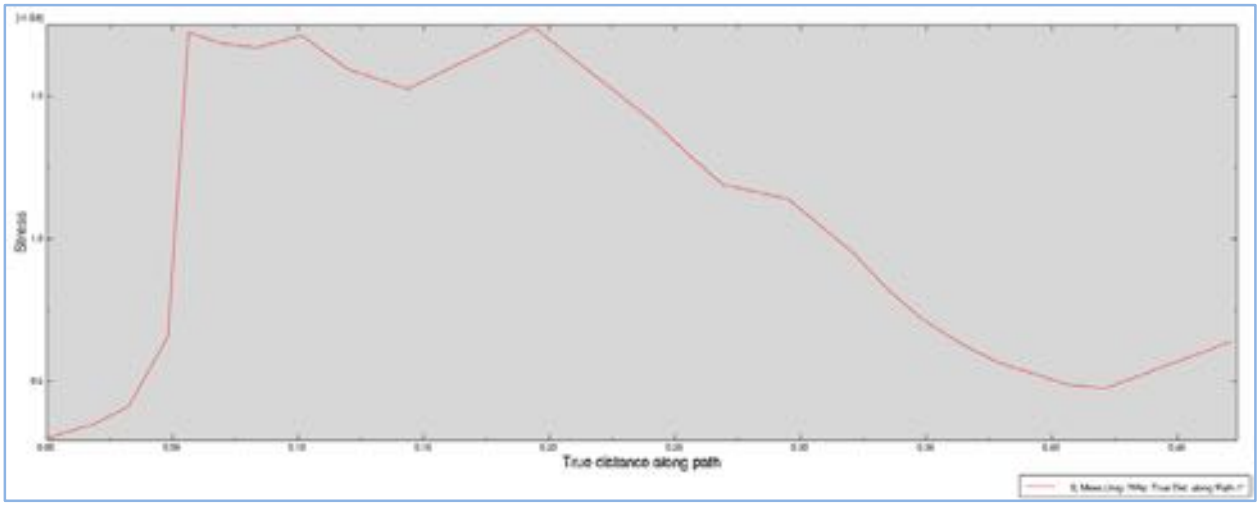

Figure 16: Corresponding stress values for the path illustrated in Figure 15.

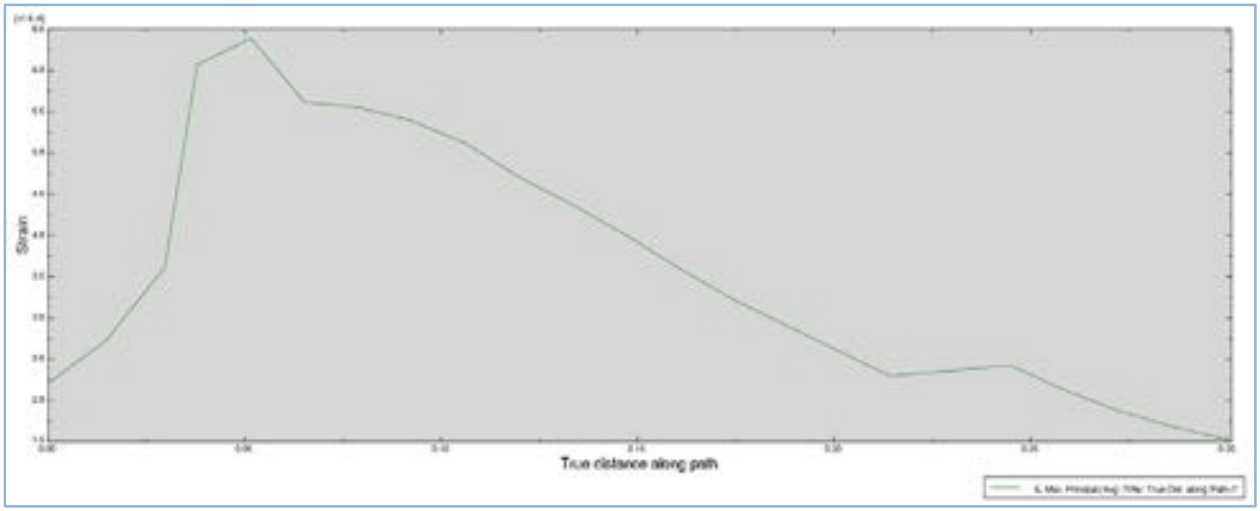

Figure 17: Corresponding strain values for the path illustrated in Figure 15.

Step/Frame

Step Name	Description
Step-1	
Step-2	

Frame

Index	Description
0	Increment 0: Base State
1	Mode 1: Value = -2.68834E-04 Freq = 0.0000 (cycles/time)
2	Mode 2: Value = -1.21223E-04 Freq = 0.0000 (cycles/time)
3	Mode 3: Value = -4.78357E-05 Freq = 0.0000 (cycles/time)
4	Mode 4: Value = 5.80304E-06 Freq = 3.83396E-04 (cycles/time)
5	Mode 5: Value = 7.28327E-05 Freq = 1.35826E-03 (cycles/time)
6	Mode 6: Value = 1.26143E-04 Freq = 1.78752E-03 (cycles/time)
7	Mode 7: Value = 1.46759E+06 Freq = 192.81 (cycles/time)
8	Mode 8: Value = 2.02367E+06 Freq = 226.41 (cycles/time)
9	Mode 9: Value = 1.22059E+07 Freq = 556.04 (cycles/time)
10	Mode 10: Value = 1.96020E+07 Freq = 704.65 (cycles/time)
11	Mode 11: Value = 2.22727E+07 Freq = 751.12 (cycles/time)
12	Mode 12: Value = 2.83241E+07 Freq = 847.03 (cycles/time)
13	Mode 13: Value = 3.65796E+07 Freq = 962.59 (cycles/time)
14	Mode 14: Value = 4.97430E+07 Freq = 1122.5 (cycles/time)
15	Mode 15: Value = 1.01296E+08 Freq = 1601.8 (cycles/time)
16	Mode 16: Value = 1.28477E+08 Freq = 1804.0 (cycles/time)
17	Mode 17: Value = 1.39275E+08 Freq = 1878.3 (cycles/time)
18	Mode 18: Value = 2.39728E+08 Freq = 2464.2 (cycles/time)
19	Mode 19: Value = 3.42377E+08 Freq = 2944.9 (cycles/time)
20	Mode 20: Value = 3.80090E+08 Freq = 3102.9 (cycles/time)
21	Mode 21: Value = 4.97824E+08 Freq = 3551.1 (cycles/time)
22	Mode 22: Value = 5.71190E+08 Freq = 3803.7 (cycles/time)
23	Mode 23: Value = 5.89752E+08 Freq = 3865.0 (cycles/time)
24	Mode 24: Value = 5.95224E+08 Freq = 3882.9 (cycles/time)
25	Mode 25: Value = 6.94769E+08 Freq = 4195.1 (cycles/time)
26	Mode 26: Value = 8.42426E+08 Freq = 4619.4 (cycles/time)
27	Mode 27: Value = 1.08060E+09 Freq = 5231.8 (cycles/time)
28	Mode 28: Value = 1.23090E+09 Freq = 5583.8 (cycles/time)
29	Mode 29: Value = 1.32255E+09 Freq = 5788.0 (cycles/time)
30	Mode 30: Value = 1.36306E+09 Freq = 5875.9 (cycles/time)
31	Mode 31: Value = 1.42915E+09 Freq = 6016.7 (cycles/time)
32	Mode 32: Value = 1.63396E+09 Freq = 6433.4 (cycles/time)
33	Mode 33: Value = 1.80947E+09 Freq = 6770.1 (cycles/time)
34	Mode 34: Value = 1.81878E+09 Freq = 6787.5 (cycles/time)
35	Mode 35: Value = 1.99517E+09 Freq = 7109.0 (cycles/time)

Figure 18: Modal analysis of the simulation.

Section 7: Summary of Major Findings

Our analysis of the results shows that the landing gear is in no danger of failing under any realistic conditions. The maximum Von Mises stress is only 6.54 MPa, while the maximum shear stress, ultimate tensile strength, and compressive yield strength of the material are all at least fifty times greater than this value. We also found that the most likely area of failure is a geometric stress concentration at the top of the landing gear fork. Essentially, the landing gear was designed with a factor of safety of at least 20.

Section 8: Works Cited

1.) G. Chauvet. (2015, January 01). Landing gear Piper Arrow IV (1st ed.) [Online]. Available: https://grabcad.com/library/landing-gear-piper-arrow-iv-1

2.) Nguyen, Thoai D., "Finite Element Analysis of a Nose Gear During Landing" (2010). *UNF*
Theses and Dissertations. Paper 215. http://digitalcommons.unf.edu/etd/215